JOURNAL OF THERMOPHYSICS AND HEAT TRANSFER
Vol. 7, No. 4, Oct.–Dec. 1993

Study of Polarization of Laser Radiation Scattered 90 Deg

D. C. Look Jr.*
University of Missouri—Rolla, Rolla, Missouri 65401
and
Y. R. Chen†
East China Institute of Technology, Nanjing, People's Republic of China

A qualitative experimental study was undertaken of the effects of spherical particle scattering on the polarization of linearly polarized He-Ne laser beams. Four concentrations of particles (either 0.22- or 0.494-μm diam) were suspended in filtered, distilled water to serve as the scattering centers. Data representing the effects of volumetric particle concentration, detector acceptance angle, cylindrical scattering volume container diameter, and detector depth are investigated. In general, large diameter particles and high particle concentrations depolarize the incident beam the most. Also, increasing the length of the path traversed by the scattered beam greatly increases the depolarization of the beam.

Nomenclature

A	=	intensity ratio, $I(\phi)/(I\phi = 0)$
C_{sca}	=	scattering cross section
c	=	effective scattering coefficient, $6C_{sca}/(\pi d^3)$
I	=	scattered intensity
I_i	=	scattered intensity for linearly polarized incident light
I_u	=	scattered intensity for unpolarized incident light
N	=	number density of scattering particles
P	=	degree of polarization
R	=	distance from scattering particle to detector, $>>\lambda$
r_0	=	particle radius
S^2	=	overall Mie scatter function
S_1	=	amplitude function for light scattered perpendicular to the scattering plane
S_2	=	amplitude function for light scattered parallel to the scattering plane
x, y, z	=	scattering coordinate system
α	=	detector optics acceptance angle
η	=	particle volume concentration
θ	=	polar scattering angle (between direction of propagation, z axis, and scatter direction)
κ	=	absorption coefficient of the scattering medium
λ	=	wavelength
τ_R	=	optical radius of the scattering volume
τ_r	=	radial or side-scatter optical thickness
τ_z	=	optical depth of the scattering volume from the surface of the scattering medium
τ_0	=	optical depth of the scattering medium in the direction of incident radiation from the surface
ϕ	=	angle of the scatter direction projected on the x-y plane
ψ	=	polar angle from the polarization direction, x axis, to the scatter direction

Introduction

SCATTERING of incident electromagnetic radiation of a prescribed polarization is becoming an important area in science and engineering. A major force driving the study of radial scatter is the characterization of missile and rocket plumes.[1–3] Identification of the plume signature is dependent on the radial scattering from particles in the plume. Radial scattering has also been used as a tool to study combustion processes.[4] Carswell and Pal[5] attempted to identify scattering particle size and multiple scattering effects from the polarization anisotropy of lidar scattering from clouds. General formulations describing multiple backscattering of polarized radiation incident on a slab of spherical particles have been given by Cheung and Ishimaru.[6] Transmitted radiation has been used as a diagnostic tool for years. For example, Cheung and Ishimaru also produced a formulation describing the effects of distributed spherical particles on the transmission of incident linearly and circularly polarized light. The dependence of reconstructed holograms on the relative orientation of polarization has been presented by Kostuk and Sincerbox.[7] Recently, El-Wakil et al.[8] have analytically described scattering from a finite, plane medium for the case of Rayleigh scattering with internal sources. In this article, a degree of polarization of the radiation emerging from the boundaries of the medium is discussed. A rigorous formalism of incoherent scatter from an opaque body in thermodynamic equilibrium is presented by Zimmerman and Dalcher.[9]

In order to understand the phenomena involved in this investigation, recall from classical physics the scattering effects for small particles (Mie theory, $d < \lambda$, e.g., Born and Wolf[10]). That is, consider a linearly polarized beam of radiation incident upon a very small particle. Figure 1a is a layout of the geometry of this situation. Note that the incoming radiation is polarized in the x-z plane where the $+z$ axis is the direction of propagation of radiant power; this is the *polarization plane*. The angle ϕ is restricted to the x-y plane, while the angles ψ and θ are the angles between the $+x$ axis and the $+z$ axis, respectively, and the scatter direction (OP). The direction OQ is the projection of OP into the x-y plane. Note that the z axis and OP (or OQ) form the *scattering plane*. Thus, for a very small particle positioned at 0, classical physics indicates that the three-dimensional scatter pattern is something like the model that is illustrated in Fig. 1b. Note that the intensity of the scattered radiation is related to the angle ψ by

$$I \propto \sin^2\psi = 1 - \sin^2\theta \cos^2\phi \qquad (1)$$

The usual discussion of scatter is highlighted by viewing the pattern of scatter in two planes. The first plane for viewing is formed by the beam polarization vector and the direction

Presented as Paper 92-2895 at the AIAA 27th Thermophysics Conference, Nashville, TN, July 6–8, 1992; received July 22, 1992; revision received Sept. 10, 1992; accepted for publication Sept. 14, 1992.

*Professor, Thermal Radiative Transfer Group, Mechanical and Aerospace Engineering and Engineering Mechanics Department. Associate Fellow AIAA.
†Visiting Scholar, Department of Optics.

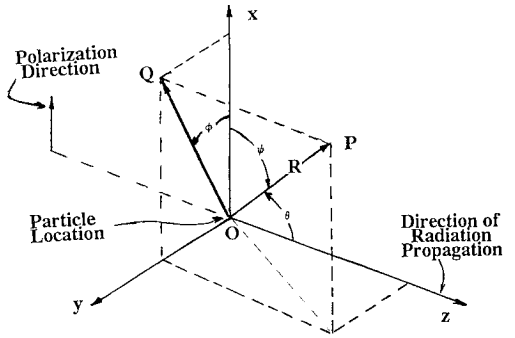

a)

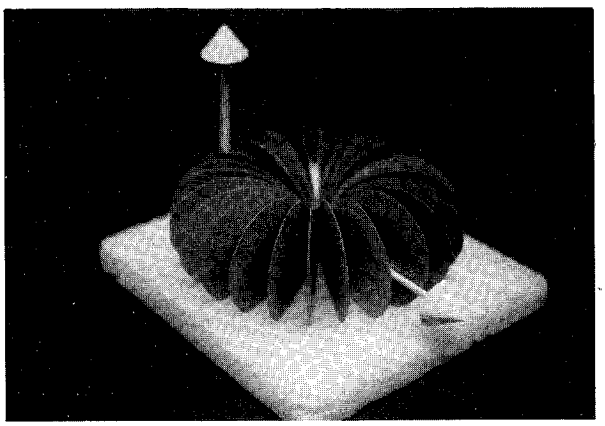

b)

Fig. 1 Geometric relationships of classical scattering: a) schematic and b) model.

of radiant power propagation; the scattering plane is the same as the polarization plane. For this situation $\phi = 0$, the scatter is restricted to the x-z plane. In this scattering plane, the intensity variation of the scattered radiation goes as the cosine squared of the angle measured from the direction of propagation ($I = \cos^2\theta$). This "figure 8" or lobed pattern may be visualized by viewing Fig. 2a. Note that this photograph is taken perpendicular to the polarization plane; hence, the figure 8 referred to is the result of cutting a plane across the toroidal-shaped scatter pattern in the plane indicated by the "arrows" in this figure.

The second popular viewing plane is perpendicular to the incident beam polarization direction (i.e., $\phi = \pi/2$ and $\psi = \pi/2$). Thus, from Eq. (1), the scattered intensity is constant with respect to the angle θ (see Fig. 2b and imagine the resultant contour by cutting the toroid shape in the plane of the photograph).

In the experiment discussed in this report, the view is somewhat different. The variation in the measured scattered intensity will be in a plane perpendicular to the direction of propagation. That is, for this case, $\theta = \pi/2$ and $\phi = \psi$. Therefore, the intensity variation is

$$I \propto \sin^2\phi \tag{2}$$

This configuration is modeled in Fig. 3, if you imagine the figure 8 contour that results by cutting the toroidal shape in a plane perpendicular to the radiant power propagation direction (i.e., the plane of the photograph).

Finally, a few words are needed about the interpretation of the experimental data based upon the classical physics description. Thus, if a linearly polarized laser beam is incident on a container of very small spherical particles, the resultant radial scattering from a particle should produce the pattern of scattering along the lines of Eq. (2), since the viewing is done in the plane perpendicular to the direction of radiant power propagation. Data acquired in a plane perpendicular to this direction should vary with ϕ. If, on the other hand, other scatter particles in this plane intercept the radiation

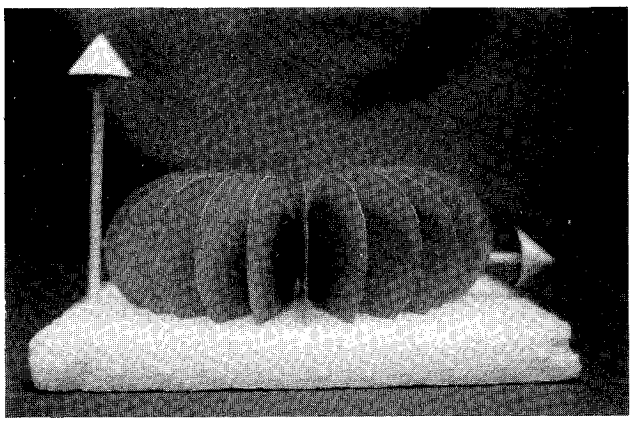

a)

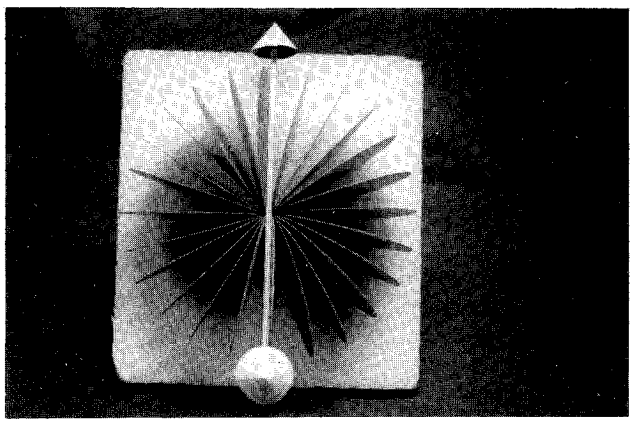

b)

Fig. 2 Classical views of scattering using the model: a) viewing perpendicular to the polarization plane and b) viewing in the polarization plane perpendicular to the direction of radiation propagation.

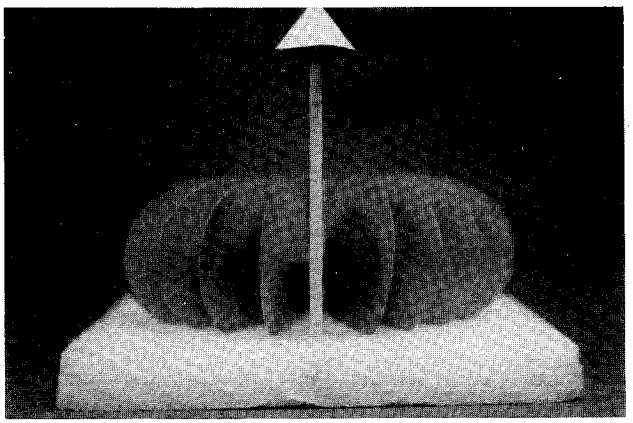

Fig. 3 Nonclassical view of scattering (viewing in the direction of radiation propagation).

scattered from the first particle, there will be further scattering which will reduce the variation in the detected radiant power intensity with the angle ϕ. This is saying that the effect of the high particle concentration in the scattering medium is highlighted by a reduction in the angular variation of the scattered radiant power with ϕ. That is, the large figure 8 variation in the detected radiant power represents the situation where the scattering particle concentration have little effect on the polarization of the incident laser beam in the plane perpendicular to the direction of propagation; thus, there is very little depolarization. On the other hand, if the detected intensity has little variation with the angle ϕ, there is a great deal of depolarization produced by the small scattering particles in this plane. That is, the multiple scattering averages the intensity in all directions.

Therefore, the purpose of this article is to present the findings of a study of scattering from spherical particles in a laboratory environment. In particular, data representing the total scattering at 90 deg from the laser beam ($\theta = \pi/2$) for all azimuth angles ($0 \leq \phi \leq 2\pi$) will be presented for the condition that the incident laser beam is linearly polarized. Furthermore, a degree of polarization is defined and calculated from the data.

Background

In order to relate the work presented in this report to the classical far-field Mie theory, return to Fig. 1. According to the single-scattering description of Mie theory, the intensity of radiation scattered to point P from a particle of radius r_0, which is subjected to unpolarized incident radiation, is

$$I_u = (\lambda^2/4\pi^2R^2)|S|^2 \tag{3}$$

where $|S|^2 = |S_1|^2 + |S_2|^2$. S_1 and S_2 are amplitude functions of the scattered radiation in a plane which is perpendicular to the scattering plane (Fig. 2b) and parallel to this plane (Fig. 2a), respectively. Explicit mathematical expressions for S_1 and S_2, which depend upon ϕ, n, r_0, etc., may be found in many optics books, including Refs. 10–12. These amplitudes may be used to define P at any point, as the ratio

$$P = [(|S_1|^2 - |S_2|^2)/(|S_1|^2 + |S_2|^2)] \tag{4}$$

For this report, the incident laser radiation is linearly polarized. The corresponding variation of the radiation scattered in a plane perpendicular to the propagation direction is[11,12]

$$I_i = (\lambda^2/4\pi^2R^2)(|S_1|^2 \sin^2\phi + |S_2|^2 \cos^2\phi) \tag{5}$$

Note that for this discussion, θ is restricted to ($\pi/2$), and therefore $|S_1|^2$ and $|S_2|^2$ are constants. So Eq. (5) may be written in a different form

$$\begin{aligned} I_i &= (\lambda/4\pi^2R^2)[(|S_1|^2 - |S_2^2|)\sin^2\phi + |S_2|^2] \\ &= PI_u \sin^2\phi + (\lambda^2/4\pi^2R^2)|S_2|^2 \end{aligned} \tag{6}$$

Thus, the expected scatter pattern when viewed perpendicular to the scattering plane (backscatter) will be of the form of a lobed, figure 8 or "bow tie" shape (i.e., $C_1 + C_2 \sin^2\phi$, C_1 and C_2 constants).

In order to investigate the degree of polarization, a ratio, based upon Eq. (6), may be used. That is, consider the ratio

$$\begin{aligned} \frac{I_i(\phi)}{I_i(\phi = 0)} &= 1 + \left(\frac{|S_1|^2}{|S_2|^2} - 1\right)\sin^2\phi \\ &= A(\phi) \end{aligned} \tag{7}$$

Then

$$|S_1|^2 = \left[\frac{A(\phi) - 1}{\sin^2\phi} + 1\right]|S_2|^2$$

Using the definition, Eq. (4) reduces to

$$P = \frac{A(\phi) - 1}{A(\phi) - 1 + 2\sin^2\phi} \tag{8}$$

At this point, it should be noted that in the following presentation of data, $A(\phi)$ and $\sin^2\phi$ should vary such that P is constant.

Optical Depth

Although not a point of emphasis in this report, but worthy of note, are the optical thicknesses involved. That is, optical thickness has a major effect on scattering and polarization of the detected laser radiation. In this study, the radial and depth optical thicknesses are not discussed in detail; they are, however, defined as

$$\tau_r = (NC_{sca} + \kappa)r = (\eta c + \kappa)r \leq \tau_R \tag{9}$$

$$\tau_z = (NC_{sca} + \kappa)z = (\eta c + \kappa)r \leq \tau_0 \tag{10}$$

Reference 3 presents a discussion of the theoretical effects of τ_r and τ_z on the radially scattered radiation. It does not, however, discuss the azimuthal (ϕ) variation on the detected polarization. In fact, the literature in this area is very sparse, even when multiple scattering is involved. Thus, a great deal of theoretical work must be done in this area.

Experimental Setup

This experimental setup was designed to measure the radiative side-scattering of a linearly polarized laser beam incident on a liquid scattering medium. This measured intensity of side-scatter is a function of scattering particle size and the concentration of particles in the liquid carrier, the diameter of the cylindrical scatter volume, and the depth of the measurement position just outside of the scatter volume. These measurements were made through the use of a fiber optics bundle that is rotated about the cylindrical scattering volume. The restricted aperture end of the bundle is set to directly view the side of the laser beam at all angular positions, i.e., $\theta = \pi/2$ and $0 \leq \phi \leq 2\pi$. The other end of the cable is connected to the detector—a photomultiplier.

Experimental Procedure

The following is a list of procedures that were used while setting up the experimental apparatus that is illustrated in Fig. 4:

1) The structure was placed on vibration isolation pads and leveled so that the level of the liquid in the container and the beam from the laser were orthogonal.

2) One of four aperture sizes were attached to the end of an optical fiber bundle to limit α. The acceptance angle of these apertures are two, three, four, and five deg, respectively. The other end of the fiber optic bundle is connected to a housed and cooled photomultiplier tube.

3) The laser was positioned so that its beam was not only perpendicular to the liquid surface, but colinear with the axis of rotation of the detector. Thus, the fiber optics bundle was positioned so as to view the side of the laser beam at all angular positions.

4) The container was thoroughly cleaned inside and out with acetone and then with distilled water to remove any particles or other foreign matter which might interfere with the scattering of interest.

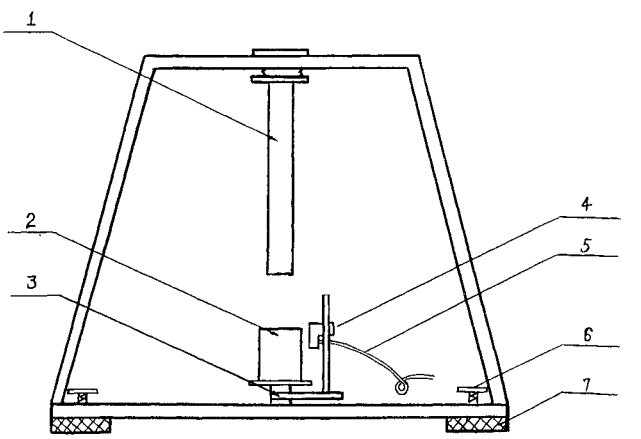

Fig. 4 Experimental apparatus: 1, laser; 2, container of liquid; 3, rotating plate; 4, vertical locator; 5, fiber optics bundle; 6, leveling screw; and 7, shock-absorbing pads.

Table 1 Optical thickness of the container of spherical scattering particles in distilled water for $\lambda = 0.6328$ μm

	0.22 μm		0.494 μm	
	τ_0	τ_R	τ_0	τ_R
0.05	34.18	6.500 (14.65)	126	24.00 (54.00)
0.025	17.09	3.290 (7.320)	63	12.00 (27.00)
0.0125	8.540	1.625 (3.660)	31.5	6.000 (13.50)
0.0005	0.342	0.065 (0.146)	1.26	0.240 (0.540)

Unbracketed numbers in the τ_R columns are for 4-cm-diam container, while bracketed numbers are for 9-cm-diam container.

5) Various amounts of 10% solution of spherical latex particles were mixed with the distilled water to serve as the scattering medium. The concentrations used in these experiments were 0.05, 0.025, 0.0125, and 0.0005% by volume (see Table 1 for the pertinent optical depths and radii).

6) The aperture tubes attached to the end of the fiber optics bundle were positioned right next to the outer surface of the container looking directly at the side of the beam.

7) The experiment was conducted in a dark room.

8) An arbitrarily selected 0-deg point around the side of the container (horizontally) was obtained by positioning the fiber optics bundle aperture such that a minimum output value was obtained. The aperture was then rotated around the container, taking measurements at prescribed intervals (usually every 15 deg in this experiment).

The steps listed above were executed for all four of the concentrations, two sizes of scatter particle diameters, two scattering container sizes, various depths of the detector probe, and four apertures that were used in this experiment. In addition, tests were run to ensure that the response of the detector system was, in fact, linear, over the range of voltages (intensity) recorded. Thus, when appropriately zeroed (as was done in this experiment), the side-scattered intensity is directly proportional to the recorded voltage and a ratio of intensities is equal to a ratio of voltages.

Experimental Results

Figures 5 and 6 present typical data for the various concentrations of the spherical scattering particles (two diameters, 0.22 or 0.494 μm, respectively). These figures appear to clearly illustrate the effect of scattering on the linear polarization of the incident laser beam. In these figures the ordinate is the ratio of the intensity of side-scatter (as a function of the angle ϕ) and the minimum for each case. These figures indicate that when the concentration of particles is small, the variation of the intensity of side-scatter is very large. Thus, the larger the ratio, the more evident the variation in the intensity of the side-scattered laser radiation and the smaller the depolarization of the beam. It is quite clear that the ratio for the 0.0005% solution exhibits the largest variation, even if its scattering intensity is smaller than that of other solutions, and therefore, depolarizes the beam the least. Table 2 presents estimates of the variation in P with angle ϕ for both particles. These values are estimates, because Eq. (8) was formulated under the assumption of single-scattering. This more than likely is not the case. Even so, this presentation dramatically portrays the depolarization by scattering of the incident laser beam as a function of particle concentration, since the magnitude of P goes down as the particle concentration increases and remains essentially constant for near single-scattering situations.

Figure 7 illustrates the effect of detector depth on the radiative side-scattering. It is clear that the maximum variation occurs near the liquid surface (almost zero depth). In fact,

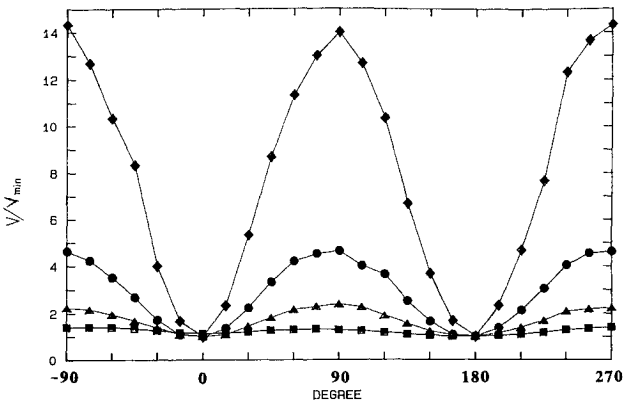

Fig. 5 Intensity ratio for the side-scatter vs scatter angle for particle with a diameter of 0.22 μm. ♦, 0.0005%; ●, 0.0125%; ▲, 0.025%; and ■, 0.05%. The acceptance angle is 2 deg, the diameter of the container is 4 cm, and the detector depth is 0.

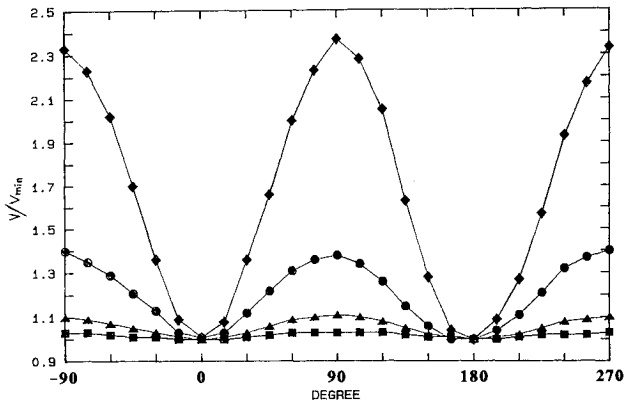

Fig. 6 Intensity ratio of the side-scatter vs scatter angle for particle with a diameter of 0.494 μm. ♦, 0.0005%; ●, 0.0125%; ▲, 0.025%; and ■, 0.05%. The acceptance angle is 2 deg, the diameter of the container is 4 cm, and the detector depth is 0.

Table 2 Estimated degree of polarization using Eq. (8) for scattering from 0.22- and 0.494-μm particles (see Figs. 5 and 6)[a]

%	ϕ = 90	75	60	45	30	15	0
0.220-μm Particles (α = 2 deg, depth = 0, D = 4 cm)							
0.05	0.1667	0.1801	0.2105	0.2537	0.3421	0.5443	——
0.025	0.3827	0.3833	0.3877	0.3975	0.4253	0.3738	——
0.0125	0.6454	0.6345	0.6269	0.6269	0.5902	0.3738	——
0.0005	0.8695	0.8621	0.8614	0.8796	0.8571	0.8334	——
0.494-μm Particles (α = 2 deg, depth = 0, D = 4 cm)							
0.05	0.0148	0.0106	0.0131	0.0099	0.0196	0.0074	——
0.025	0.0476	0.0460	0.0458	0.0472	0.0566	0.0694	——
0.125	0.1667	0.1579	0.1620	0.1735	0.2063	0.1829	——
0.0005	0.4065	0.3972	0.4047	0.4117	0.4186	0.4018	——

[a]Note: "0" depth means that the probe was positioned just below the surface level at a depth such that the bottom side of the surface was not "seen" by the detector for the acceptance angle of the detector; this corresponded to the maximum reading for the run. In each case the maximum variation occurs near the actual surface, but not at the position where the aperture is split by the plane of the surface.

the farther down from the top of the liquid the detector is positioned, the less is the variation in the detected intensity of scattered light. Figure 8 presents the same information for a different particle size. Table 3 presents the variation in the estimated degree of polarization with depth.

Figure 9 is a comparison of the effects of the aperture acceptance angle. The larger the acceptance angle of the aperture, the larger is the variation in the magnitude of the intensity detected. Actually, this observation is misleading in that the relative variation (V_{max}/V_{min}) is approximately the

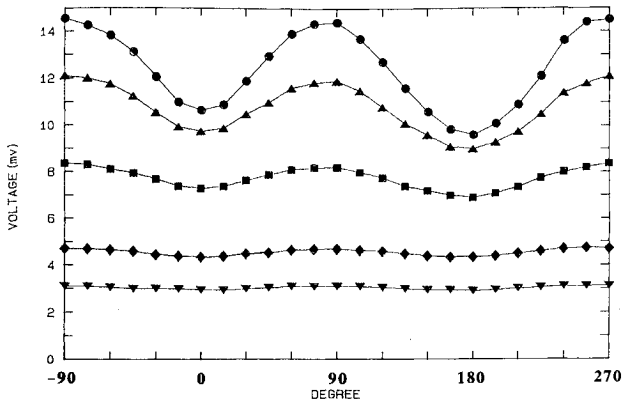

Fig. 7 Side-scattered intensity from 0.22-μm particles vs scatter angle with detector depth as the parameter: ●, 0 cm; ▲, 0.64 cm; ■, 1.27 cm; ♦, 1.91 cm; and ▼, 2.54 cm. The acceptance angle is 5 deg, the concentration is 0.05%, and the container diameter is 4 cm.

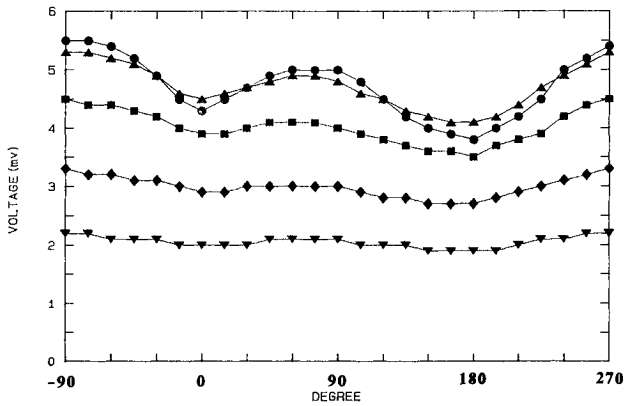

Fig. 8 Side-scattered intensity from 0.22-μm particles vs scatter angle with detector depth as the parameter: ●, 0 cm; ▲, 0.64 cm; ■, 1.27 cm; ♦, 1.91 cm; and ▼, 2.54 cm. The acceptance angle is 2 deg, the concentration is 0.05%, and the container diameter is 4 cm.

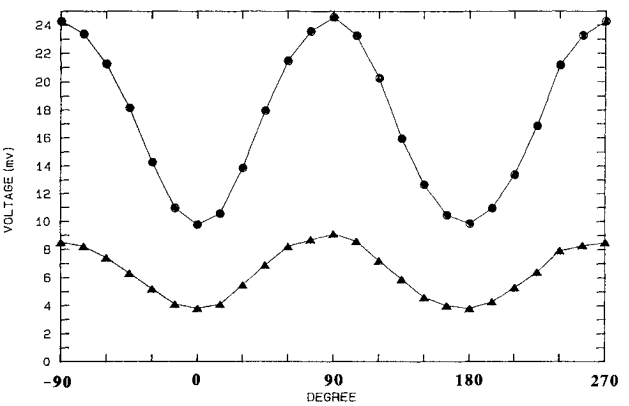

Fig. 9 Side-scattered intensity vs scatter angle from 0.22-μm particles with the acceptance angle as the parameter; ●, 5 deg and ▲, 2 deg. The concentration is 0.025%, the detector depth is 0, and the container diameter is 4 cm.

same regardless of the acceptance angle. Table 4 presents the estimated degree of polarization variation with ϕ per the acceptance angle. Note that for these data the accepted intensity variation across the aperture is not significant, since the circular area seen by the detector at the laser beam position is 0.035-cm (0.079-cm) for the 4-cm (9-cm) diam container.

Figure 10 indicates the effects of the diameter of the scatter medium container. The scatter intensity variation for the smaller

Table 3 Estimated degree of polarization using Eq. (8) for scattering from 0.22- and 0.494-μm particles (see Figs. 7 and 8)

$z\backslash\phi$	90	75	60	45	30	15	0
0.22-μm Particle (α = 5 deg, 0.0005%, D = 4 cm)							
0	0.2050	0.2060	0.2258	0.2672	0.3333	0.1346	——
0.25	0.1346	0.1296	0.1176	0.1089	0.1176	0.0076	——
0.5	0.0861	0.0787	0.0759	0.0676	0.0799	0.0976	——
0.75	0.0387	0.0413	0.0439	0.0543	0.0439	0.0790	——
1.0	0.0333	0.0356	0.0333	0.0333	0.0333	0.1140	——
0.22-μm Particles (α = 2 deg, 0.0005%, D = 4 cm)							
0	0.1244	0.1119	0.1038	0.0894	0.0675	0.0189	——
0.25	0.0754	0.0669	0.0537	0.0397	0.0284	0.0054	——
0.5	0.0588	0.0522	0.0391	0.0244	0.0109	0.0021	——
0.75	0.0471	0.0359	0.0306	0.0180	0.0284	0.0266	——
1.0	0.0380	0.0274	0.0239	0.0206	0.0206	0.0378	——

Table 4 Estimated degree of polarization using Eq. (8) for scattering from 0.22-μm particles (see Fig. 9) for a 0.0025% solution, 0 depth and d = 4 cm

$\alpha\backslash\phi$	90	75	60	45	30	15	0
2 deg	0.4108	0.4036	0.3736	0.3559	0.2962	0.2820	——
5 deg	0.4252	0.4265	0.4389	0.4615	0.4787	0.4775	——

Table 5 Estimated degree of polarization using Eq. (8) for scattering from 0.22-μm particles (see Fig. 10) for a 0.0025% solution, α = 2 deg, and depth = 0

$D\backslash\phi$	90	75	60	45	30	15	0
40 mm	0.4108	0.4036	0.3736	0.3559	0.2962	0.2820	——
90 mm	0.1184	0.1258	0.1260	0.1354	0.1410	0.0527	——

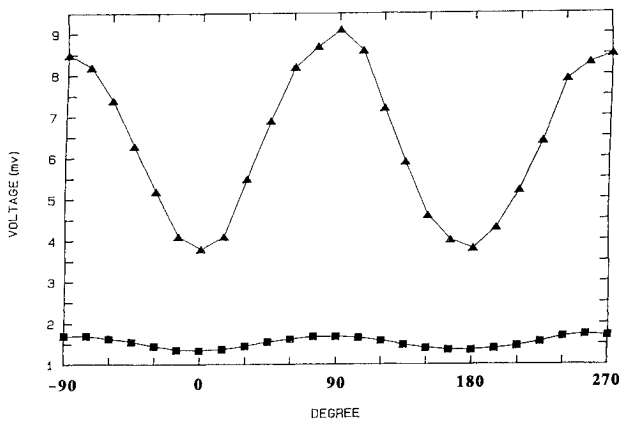

Fig. 10 Side-scattered intensity from 0.22-μm particles vs scatter angle with container or scatter volume diameter as parameter; ▲, 40 mm and ■, 90 mm. The acceptance angle is 2 deg, the concentration is 0.025%, and the detector depth is 0.

diameter container is much larger than that of the larger diameter container because of the reduced light propagation distance in the scattering medium. Table 5 presents the estimated degree of polarization values with ϕ per scatter medium diameter.

Figures 11 and 12 are side-by-side comparisons of the variations in scattered intensity for the two sizes of particles used, 0.22 and 0.494-μm diam. Both of these figures illustrate the typical variation regardless of concentration; in side-scattering, the variation in the intensity per particle concentration is larger for the smaller particles. The variation with 0.22-μm-diam particles is larger than that with 0.494-μm-diam particles for all concentrations.

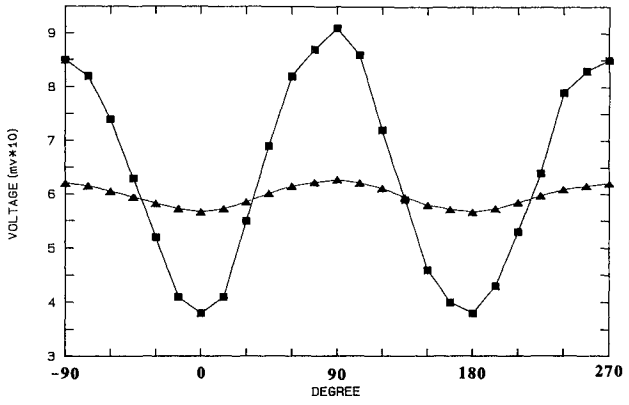

Fig. 11 Comparison of the variation in the side-scatter intensity as a function of angle with particle size as the parameter for a 0.025% solution; ■, 0.22 μm and ▲, 0.494 μm. The container diameter is 4 cm, detector depth is 0, and the acceptance angle is 2 deg.

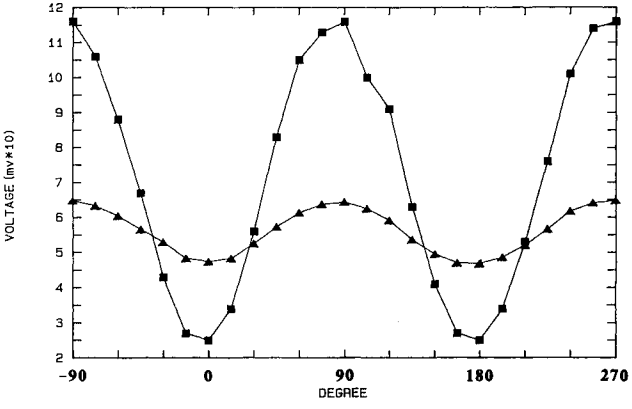

Fig. 12 Comparison of the variation in the side-scatter intensity as a function of angle with particle size as the parameter for the 0.0125% solution; ■, 0.22 μm and ▲, 0.494 μm. The container diameter is 4 cm, depth is 0, and the acceptance angle is 2 deg.

Conclusions

The following is a list of conclusions that may be drawn from the information presented in this study:

1) The effect of scattering on the linear polarization of the detected beam is quite pronounced as the particle concentration of the scattering medium decreases. When the concentration is large, the variation in the side-scatter (with angle) is small and becomes very nearly constant. Thus, in these cases, the scattering effect on the polarization of the detected beam is almost complete (see Figs. 5 and 6).

2) The variation in intensity of radiative side-scattering decreases as the detector position moves down from the top surface of the liquid (see Figs. 7 and 8).

3) Larger detector acceptance angles indicate larger variations in the magnitude of the measured side-scatter intensity for a given concentration of solution (see Fig. 9).

4) For the same particle concentrations, the effects of the variation in the scattered radiant process is more pronounced when using small diameter containers (see Fig. 10).

5) For all particle concentrations tested, both the variation in the intensity of side-scattered radiation and, thus, the effects on the linear polarization of the scattered laser beam, are more evident with the 0.22-μm-diam particles than with 0.494-μm-diam particles (see Figs. 11 and 12).

6) The manipulation of the data using $A(\phi)$ and P appears to be a viable means with which to study scattering effects on the polarization of the incident beam.

Acknowledgment

The authors acknowledge the partial support of the National Science Foundation (NSF) through Grant CTS-9103971.

References

[1]Nelson, H. F., "Influence Particulates on Infrared Emission from Tactical Rocket Exhausts," *Journal of Spacecraft and Rockets*, Vol. 21, No. 5, 1984, pp. 425–432.

[2]Nelson, H. F., "Influence of Scattering on Infrared Signatures of Rocket Plumes," *Journal of Spacecraft and Rockets*, Vol. 21, No. 5, 1984, pp. 508–510.

[3]Nelson, H. F., and Satish, B. V., "Radial Scattering of Laser Beam in Anisotropic Scattering Media," *Journal of Thermophysics and Heat Transfer*, Vol. 2, No. 2, 1988, pp. 104–109.

[4]Johnston, S. C., Dibble, R. W., Schefer, R. W., Ashurst, W. T., and Kollmann, W., "Laser Measurements and Stochastic Simulations of Turbulent Reacting Flows," *AIAA Journal*, Vol. 24, No. 6, 1986, pp. 918–937.

[5]Carswell, A. I., and Pal, S. R., "Polarization Anisotropy in Lidar Multiple Scattering from Atmospheric Clouds," *Applied Optics*, Vol. 24, No. 21, 1985, pp. 3464–3471; see also *Applied Optics*, Vol. 19, No. 24, 1980, pp. 4123–4125.

[6]Cheung, R. L.-T., and Ishimaru, A., "Transmission, Backscattering, and Depolarization of Waves in Randomly Distributed Spherical Particles," *Applied Optics*, Vol. 21, No. 20, 1982, pp. 3792–3798.

[7]Kostuk, R. K., and Sincerbox, G. T., "Polarization Sensitivity of Noise Recorded in Silver Halide Volume Holograms," *Applied Optics*, Vol. 27, No. 14, 1988, pp. 2993–2998.

[8]El-Wakil, S. A., Madkour, M. A., and Abulwafa, E. M., "Polarized Radiative Transfer in an Aerosol Medium," *Journal of Quantitative Spectroscopy and Radiative Transfer*, Vol. 46, No. 6, 1991, pp. 523–529.

[9]Zimmerman, E. C., and Dalcher, A., "Incoherent Radiative Properties of an Opaque Body," *Journal of the Optical Society of America A*, Vol. 8, No. 12, 1991, pp. 1947–1954.

[10]Born, M., and Wolf, E., "Principles of Optics," 4th ed., Pergamon, New York, 1970, pp. 633–656.

[11]Van De Hulst, H. C., "Light Scattering by Small Particles," Wiley, New York, 1957, p. 127.

[12]Kerker, M., "The Scattering of Light and Other Electromagnetic Radiation," Academic Press, New York, 1969, p. 35.